Cell, Vol. 105, 379–389, May 4, 2001, Copyright ©2001 by Cell Press

# Specificity Determinants in Phosphoinositide Dephosphorylation: Crystal Structure of an Archetypal Inositol Polyphosphate 5-Phosphatase

**Yosuke Tsujishita,[1] Shuling Guo,[2] Leslie E. Stolz,[2] John D. York,[2] and James H. Hurley[1,3]**
[1] Laboratory of Molecular Biology
National Institute of Diabetes and Digestive and Kidney Diseases
National Institutes of Health
Bethesda, Maryland 20892
[2] Howard Hughes Medical Institute
Department of Pharmacology and Cancer Biology
Duke University Medical Center, DUMC 3813
Durham, North Carolina 27710

## Summary

**Inositol polyphosphate 5-phosphatases are central to intracellular processes ranging from membrane trafficking to $Ca^{2+}$ signaling, and defects in this activity result in the human disease Lowe syndrome. The 1.8 Å resolution structure of the inositol polyphosphate 5-phosphatase domain of SPsynaptojanin bound to $Ca^{2+}$ and inositol (1,4)-bisphosphate reveals a fold and an active site His and Asp pair resembling those of several $Mg^{2+}$-dependent nucleases. Additional loops mediate specific inositol polyphosphate contacts. The 4-phosphate of inositol (1,4)-bisphosphate is misoriented by 4.6 Å compared to the reactive geometry observed in the apurinic/apyrimidinic endonuclease 1, explaining the dephosphorylation site selectivity of the 5-phosphatases. Based on the structure, a series of mutants are described that exhibit altered substrate specificity providing general determinants for substrate recognition.**

## Introduction

Inositol phosphates are among the most widespread second messenger molecules in eukaryotic cell signaling (Berridge and Irvine, 1989; Majerus, 1992; Liscovitch and Cantley, 1994). Inositol-derived messengers can be divided into two general classes, which are either water-soluble or lipids. Lipid-derived molecules phosphorylated at the D-3, 4, and 5 positions, singly and in all possible combinations, are present in eukaryotic cells and each has a distinct regulatory role (De Camilli et al., 1996; Rameh and Cantley, 1999; Odorizzi et al., 2000). The levels of these signaling molecules are regulated by their phosphorylation by lipid kinases and dephosphorylation by lipid phosphatases. Hydrolysis of certain inositol phospholipids by phospholipase C results in water soluble inositol phosphates that are further metabolized by a number of kinases and phosphatases (Majerus, 1992; Shears, 1998; Odom et al., 2000).

The inositol 5-phosphatases are a family of enzymes (Figure 1) that play a central role in signaling through both soluble and lipid inositol phosphates by catalyzing the specific hydrolysis of the 5-phosphoryl group (Mitchell et al., 1996; Drayer et al., 1996; Woscholski and Parker, 1997; Majerus et al., 1999). These enzymes share a requirement for a divalent metal ion, and have been predicted based on sequence analysis to be similar in fold and mechanism to DNase I and related metal-dependent phosphohydrolases (Dlakic, 2000; Whisstock et al., 2000). Over ten mammalian and four yeast genes have been shown to encode 5-phosphatase activity that may be grouped according to their substrate selectivity (Majerus et al., 1999). For example, type I 5-phosphatases only hydrolyze soluble inositol phosphates, whereas type II enzymes are active against both soluble and lipid inositol phosphates. Within the framework of a common enzyme mechanism, these enzymes have a wide range of substrate specificities and subcellular distribution, and an equally wide range of biological roles.

Recent studies emphasize the critical roles of inositol 5-phosphatases in diverse normal and pathophysiological processes. For example, inositol phosphatase-catalyzed turnover of lipid inositol phosphates, possibly phosphatidylinositol 4,5-bisphosphate, is required for membrane trafficking as shown by studies using synaptojanin-1 deficient mice and *C. elegans* (Cremona et al., 1999; Harris et al., 2000). Inhibition of the type I 5-phosphatase, which is responsible for the hydrolysis of the second messenger inositol (1,4,5)-trisphosphate ($IP_3$), has been proposed to regulate store-operated calcium influx (Hermosura et al., 2000). Certain diseases are associated with genetic deficiences affecting 5-phosphatases. The Lowe oculocerebrorenal syndrome (OCRL) is an X-linked disorder characterized by congenital cataracts, mental retardation, and renal Fanconi syndrome. The *OCRL1* gene encodes a 5-phosphatase that is deficient in ORCL patients (Attree et al., 1992; Suchy et al., 1995; Zhang et al., 1995). Among the mutations reported in OCRL patients are many missense mutations within the 5-phosphatase catalytic domain.

Production of phosphatidylinositol (3,4,5)-trisphosphate ($PIP_3$) by phosphoinositide 3-kinase (PI3K) is central to signaling through the insulin receptor. Mice lacking the *SHIP2* gene, a 5-phosphatase that preferentially dephosphorylates 3-phosphoinositides, are hypoglycemic and sensitized to insulin (Clement et al., 2001). Since insulin resistance is a central aspect of adult onset (type II) diabetes, the sensitization of *SHIP2* −/− and +/− mice to insulin suggests that SHIP2 may be a potential therapeutic target for the treatment of type II diabetes (Clement et al. 2001).

In order to obtain three-dimensional structural information on the inositol 5-phosphatase catalytic (IPP5C) domain at high resolution, we subcloned and screened a variety of 5-phosphatases for high-level expression of recombinant protein and subsequent crystallization. Success was obtained with a previously uncharacterized putative 5-phosphatase deduced from the sequence of *Schizosaccharomyces pombe* chromosome

[3] Correspondence: jh8e@nih.gov

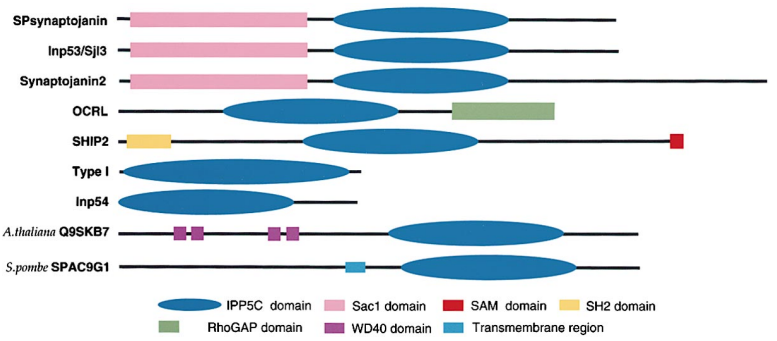


Figure 1. Domain Structures of Representative 5-Phosphatases

The catalytic IPP5C domain is indicated by a blue ellipse. Domain structure information and IPP5C domain boundaries were obtained from SMART (Schultz et al., 1998) and Pfam (Bateman et al., 1999).

II. The protein is one of three predicted inositol polyphosphate 5-phosphatases found to date in the *S. pombe* genome. BLAST searches (Altschul et al., 1997) revealed that the coding sequence of the *S. pombe* protein shares the tripartite domain structure found in the dual-functional class of inositol lipid phosphatase proteins, mammalian synaptojanin and the *Saccharomyces cerevisiae* counterparts Inp52 and Inp53, also referred to as Sjl2 and Sjl3 for their structural similarity to synaptojanin (McPherson et al., 1996; Srinivasan et al., 1997; Stolz et al., 1998). This class of proteins has an amino-terminal Sac1-like domain that encodes a polyphosphoinositide phosphatase activity (PPIPase), a central 5-phosphatase domain that typically prefers $PI(4,5)P_2$ substrates, and a carboxy-terminal proline rich region (Guo et al., 1999). We therefore refer to it as SPsynaptojanin for *S. pombe* synaptojanin. Here, we report the enzymatic characterization of the IPP5C domain of SPsynaptojanin (comprising residues 534–880), its crystal structure alone at 2.0 Å resolution and in a product complex with inositol (1,4)-bisphosphate and $Ca^{2+}$ at 1.8 Å resolution, and a structure/function analysis of substrate specificity and membrane binding determinants.

## Results

### Enzyme Activity and Complementation of *inp51 inp52 inp53* Triple Mutant

The inositol polyphosphate phosphatase catalytic (IPP5C) domain of SPsynaptojanin (SPsynaptojanin-IPP5C) is highly active against a range of soluble and lipid inositol phosphates (Figure 2). The enzyme is active in dephosphorylating the 5-position of $Ins(1,4,5)P_3$ and $Ins(1,3,4,5)P_4$ and to a lesser extent $Ins(1,4,5,6)P_4$. The enzyme is also active against $PI(4,5)P_2$ presented in sonicated vesicles and Triton mixed micelles, and somewhat less active against $PI(3,5)P_2$ in unilamellar vesicles. Activity against $PI(3,5)P_2$ drops sharply when this substrate is presented in mixed micelles. Furthermore, the enzyme hydrolyzes $PIP_3$ to produce $PI(3,4)P_2$. Thus, this activity profile most resembles the type II inositol 5-phosphatases. The lipid 5-phosphatase activity of SPsynaptojanin-IPP5C is functional in vivo as transformation of *inp51 inp52 inp53* triple-mutant strains of *S. cerevisiae* with a plasmid expressing the SPsynaptojanin-IPP5C domain results in rescue of cell viability (Figure 2D).

### Overall Structure

The overall architecture of the IPP5C domain consists of two lobes of the $\alpha+\beta$ type (Figure 3). The structure contains two mostly antiparallel sheets on the interior, flanked by two $\alpha$-helical layers on the outside. The IPP5C core contains a total of 7 $\alpha$ helices and 11 $\beta$ strands. The strands are arranged in the two sheets in the order 3, 4, 2, 1, 11, and 10, and 5, 6, 7, 8, and 9, respectively. All of the strands are antiparallel except for the central pair in each sheet, 1 and 2 in the first, and 7 and 8 in the second. Residues 784–785 of the $\alpha$7-$\beta$9 loop form a two-residue antiparallel sheet interaction with $\beta$9, approximating a sixth strand in sheet II. In addition to the IPP5C domain itself, the crystal structure contains N- and C-terminal extensions that are outside of the conserved core. Together, the N and C termini form an extended stalk consisting of two long helices that we designate $\alpha$N and $\alpha$C.

### $Ins(1,4)P_2$ and $Ca^{2+}$ Binding Sites

The active site of SPsynaptojanin-IPP5C is located in a funnel-shaped depression formed at one end of the two $\beta$ sheets. The active site was located by soaking crystals for 20 hr in 2 mM $Ins(1,4,5)P_3$ and 1 mM $CaCl_2$ and determining the structure by the Fourier difference technique (Figure 4). Although the crystals were soaked in $Ins(1,4,5)P_3$, the difference density indicated beyond doubt that $Ins(1,4)P_2$, and not $Ins(1,4,5)P_3$, was bound. We believe that the bound $Ins(1,4)P_2$ represents the enzymatic hydrolysis product and not a contaminant in the $Ins(1,4,5)P_3$ for two reasons. First, $Ins(1,4,5)P_3$ binds to SPsynaptojanin-IPP5C with high affinity ($K_m = 32\ \mu M$), so there is no reason to expect that $Ins(1,4)P_2$, which is not a substrate at all, would bind preferentially in the presence of both compounds. Second, a data set was obtained from a shorter soak (10 min) that yielded a complicated electron density map in the active site region (not shown) consistent with a mixture of bound $Ins(1,4,5)P_3$ and $Ins(1,4)P_2$. All available evidence suggests that SPsynaptojanin-IPP5C as crystallized is catalytically active and that the complex described is that of the reaction product.

$Ins(1,4)P_2$ has approximate 2-fold symmetry, but the predominant binding mode was determined unambiguously from the high quality of the 1.8 Å electron density map (Figure 4) for the complex structure. The 1-phosphoryl moiety interacts with the main chain NH groups of residues 704 and 705 from the $\beta$7-$\alpha$4 loop (Figure 4).

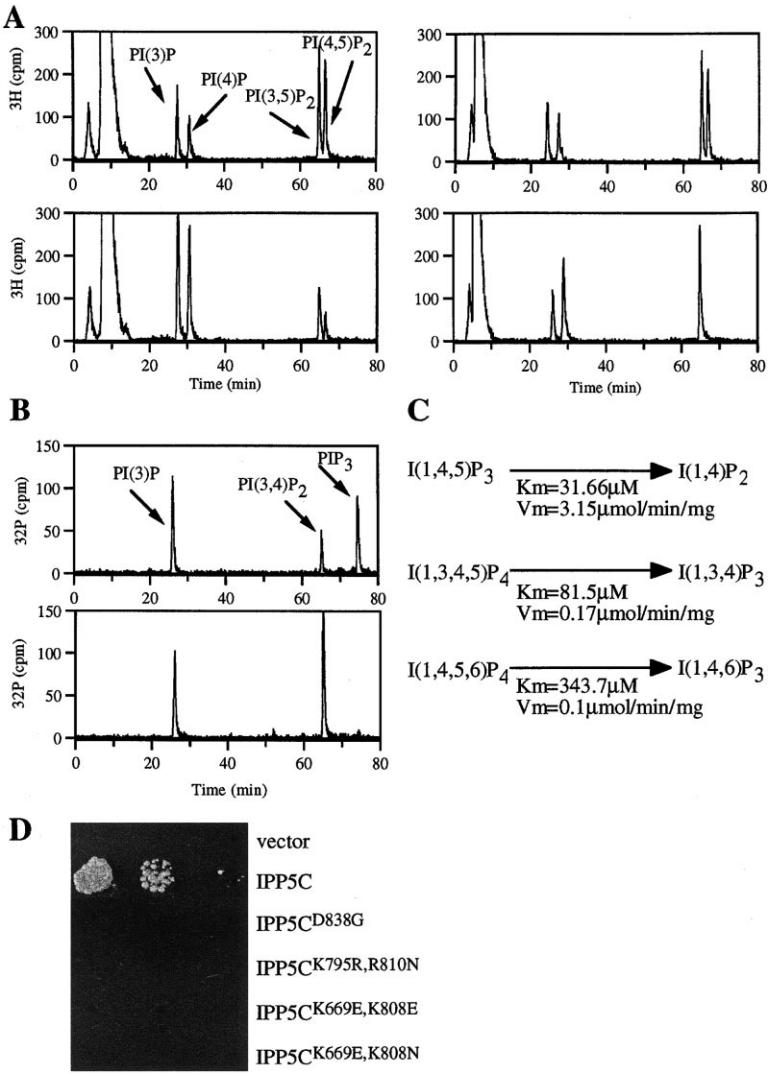


Figure 2. Enzymatic and In Vivo Characterization of IPP5C Domain of SPsynaptojanin

(A) SPsynaptojanin-IPP5C activity against [$^3$H]-*myo*-inositol-labeled yeast substrate. SPsynaptojanin-IPP5C was incubated with mixed-vesicle substrate (without detergent) or detergent-micelle substrate (0.2% Triton X-100). The assay product was deacylated and analyzed by HPLC. The panels on the left are assay product with mixed-vesicle substrate and the panels on the right are assay product with detergent-micelle substrate. Top panels are control reactions and bottom panels are SPsynaptojanin-IPP5C reactions.

(B) SPsynaptojanin-IPP5C activity against $^{32}$P-phosphate-labeled 3-phosphorylated phosphoinositides. The assay was carried out and analyzed as above, and the HPLC trace of reactions with detergent-micelle substrate is shown. The top panel is the control reaction and the bottom panel is with SPsynaptojanin-IPP5C.

(C) Biochemical parameters of SPsynaptojanin-IPP5C toward soluble inositol polyphosphates. The assays were carried out as described in Experimental Procedures.

(D) In vivo function of the SPsynaptojanin-IPP5C domain. Wild-type and mutant SPsynaptojanin-IPP5C copper-inducible yeast expression vectors were transformed into *S. cerevisiae inp51 inp52 inp53 GAL::INP53* triple mutants. Transformants were grown to saturation in media containing galactose, then serially diluted and spotted onto plates containing dextrose and 50 μM $CuSO_4$. Pictures were taken after four days at 30°C. The strains were diluted so that the spots contained approximately 250, 50, and 10 cells, from left to right.

The interaction with 704 is direct, while the interaction with 705 is water mediated. The 4-phosphoryl moiety interacts directly with three side chains, those of Tyr-794, Lys-795, and Arg-810, from the α7-β9 loop, and β9 itself, respectively. The 4-phosphoryl also has a water-mediated interaction with the Nε of the catalytic His-839 and two water-mediated interactions with the bound $Ca^{2+}$ ion. Arg-744 of the β8-α5 loop forms a hydrogen bond with the 5-hydroxyl, the only direct protein interaction with one of the inositol hydroxyl groups.

The bound $Ca^{2+}$ ion is directly coordinated by three protein ligands and four water molecules. The amide oxygen of Asn-568 (β1-α1 loop) and both carboxylate oxygens of Glu-597 (β2-α2 loop) coordinate the $Ca^{2+}$ ion. Of the four water molecules, two form bridging interactions with the 4-phosphoryl group of Ins(1,4)$P_2$, one with the side chain oxygens of Asp-566 and Asp-838, and one with the main chain carbonyl of Leu-601.

## Structural Similarities to Nucleases

We searched the Protein Data Bank for structural similarities to SPsynaptojanin-IPP5C using VAST (Gibrat et al., 1996). Very extensive structural similarities were found with the nucleases deoxyribonuclease I (DNase I; pdb entry 3dni; Suck and Oefner, 1986) and exonuclease III (exoIII, pdb entry 1ako; Mol et al., 1995). The structure of SPsynaptojanin-IPP5C can be superimposed on that of DNaseI with an rmsd of 3.5 Å over 165 Cα atoms, and on that of exoIII with an rmsd of 3.7 Å over 169 Cα atoms. The structures of a third member, the human DNA repair endonuclease APE1, have been characterized at several steps in the enzymatic reaction cycle (Gorman et al., 1997, Mol et al., 2000; Figure 5). Despite the lack of significant pairwise sequence identity, structural similarity was recently predicted on the basis of sensitive multiple sequence alignments (Dlakic, 2000; Whisstock et al., 2000), an extension of an earlier discovery of homology between the nucleases and bacterial sphingomyelinase (Matsuo et al., 1996).

## Mutagenesis

In order to gain insight into the determinants of substrate binding and selectivity, the structure was used to predict substitution mutants that would alter catalysis and spec-

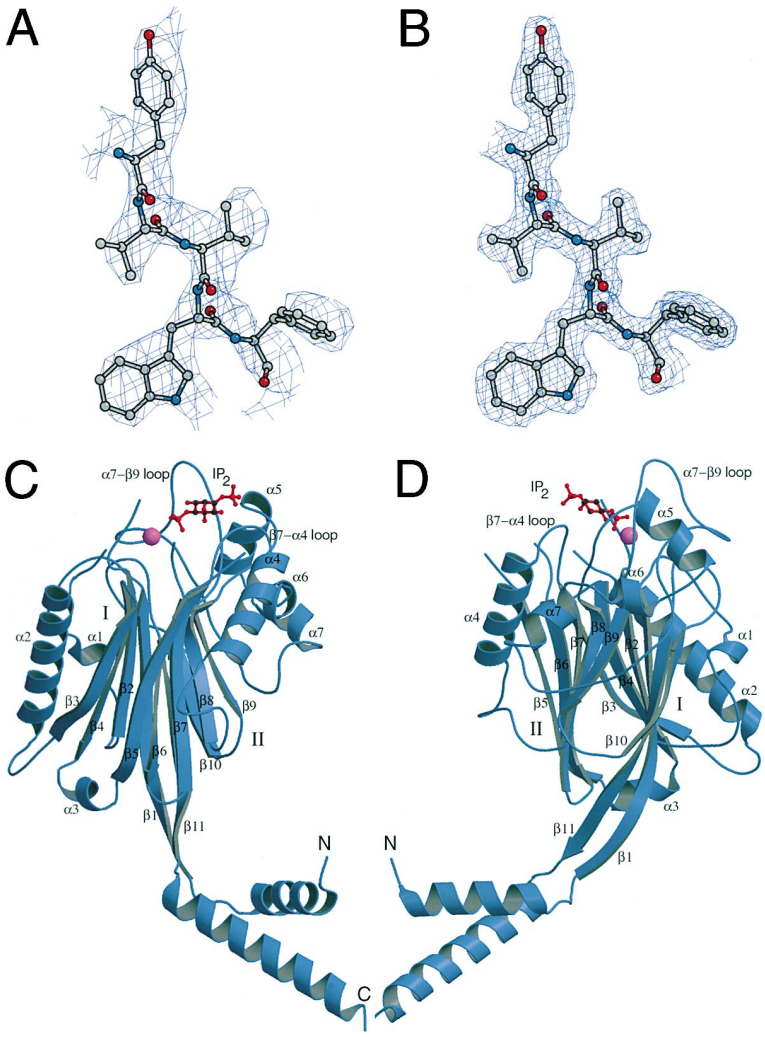


Figure 3. Structure of the IPP5C Domain of SPsynaptojanin

(A) Electron density from density-modified SIRAS map, contoured at 1.2 σ.

(B) $2F_o-F_c$ electron density from the same region of the structure, contoured at 1.2 σ.

(C) Ribbon diagram of the overall structure of SPsynaptojanin-IPP5C, together with the N- and C-terminal helical extensions, and the bound $Ca^{2+}$ ion and Ins(1,4)$P_2$ molecule from the complex structure.

(D) Diagram in (C) rotated about the y axis. Structural images were generated using Molscript (Kraulis, 1991) and Raster3D (Merritt and Bacon, 1997).

ificity. The first was a catalytically inactive mutant D838G designed as a negative control since this residue was already known to be essential in sphingomyelinase and type II 5-phosphatase (Matsuo et al., 1996, Whisstock et al., 2000). The second mutant K795R/R810N was designed to favor D-3 phosphorylated inositol phosphates, analogous to the SHIP class of 5-phosphatases. Third, a pair of mutants were designed to test whether electrostatic interactions between the enzyme membrane-proximal face and lipid bilayers are responsible for lipid versus soluble inositol phosphate specificity (K669E/K808E and K669E/K808N). The relative enzymatic activities of the mutants are shown in Table 1 and discussed in detail below. Each mutant was also tested for the ability to complement the lethal phenotype of the *inp51 inp52 inp53* triple mutant yeast strain. Although mutants were all expressed at similar levels in yeast, none of them were able to restore growth of these strains, indicating that the 5-phosphatase activity had been compromised. It is noteworthy that SPsynaptojanin-IPP5C was a relatively weak suppressor of lethality as compared to its *S. cervisiae* Inp52-IPP5C counterpart (data not shown).

## Discussion

### Catalytic Mechanism and Dephosphorylation Site Selectivity

The structure of the SPsynaptojanin IPP5C domain confirms earlier predictions of a conserved catalytic mechanism with DNase I, APE1, and related endonucleases (Dlakic, 2000; Whisstock et al., 2000). APE1 is the best-studied member of this enzyme family, as its structure is known in the apo form (Gorman et al., 1997) and in both pseudo-Michaelis and product complexes with intact and nicked DNA, respectively (Mol et al., 2000). A detailed comparison of the Ins(1,4)$P_2$ complex with the APE1 DNA complexes shows that the three-dimensional arrangement as well as the identities of the key catalytic residues and metal ligands are very similar in SPsynaptojanin-IPP5C and APE1 (Figure 5).

There are significant differences between the product binding geometries observed in the SPsynaptojanin-IPP5C/Ins(1,4)$P_2$ complex and the APE1 nicked DNA complex. In the ternary complex of APE1 with $Mn^{2+}$ and nicked DNA, the hydrolysis products can be visualized in the crystal, since presumably the presence of extensive

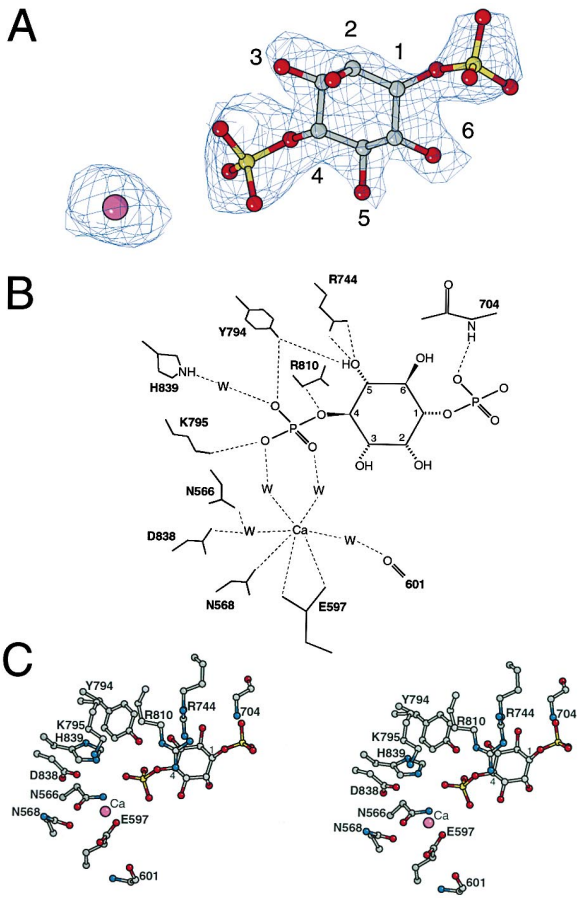


Figure 4. Inositol Phosphate Binding in the Active Site of the SPsynaptojanin-IPP5C Domain

(A) Electron density from an $(F_{obs}(soak)-F_{obs}(apo))\alpha_{calc}$ Fourier synthesis, contoured at 3 $\sigma$.

(B) Schematic of interactions in the product complex.

(C) Stereoview of interactions in the product complex, shown in the same orientation as (B).

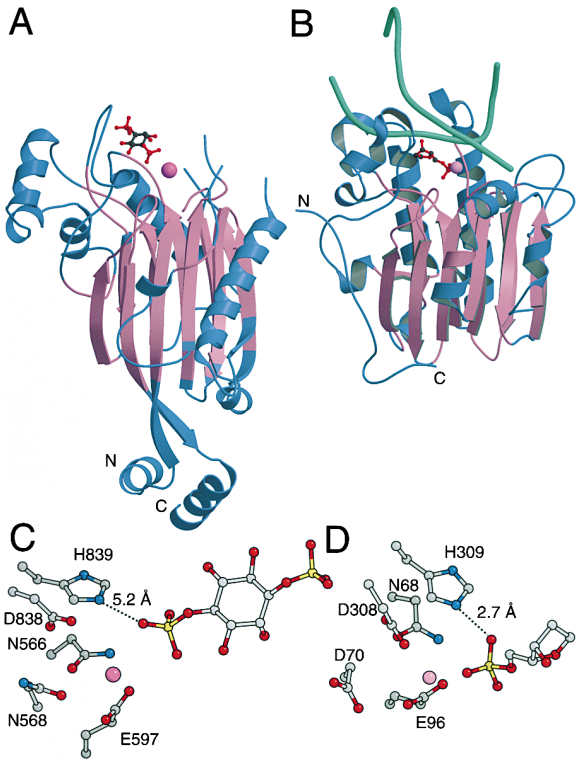


Figure 5. Comparison to APE1

(A) SPsynaptojanin-IPP5C, with regions that superimpose on APE1 colored red.

(B) APE1 complex with nicked DNA shown in green (pdb entry 1DE9, Mol et al., 2000). The proteins are colored red where the structure superimposes on SPsynaptojanin-IPP5C.

(C) Ins(1,4)$P_2$ binding to the catalytic site of SPsynaptojanin-IPP5C. Note the displacement of the 4-phosphate as compared to the scissile phosphate in the APE1/$Mn^{2+}$/scissile phosphate complex in (D).

flanking sequences on the DNA places strong constraints on the binding mode of the products. In APE1, the position of the scissile phosphate differs by only 0.7 Å between the pseudo-Michaelis and the product complex. The 5-phosphatase reaction products of Ins(1,4,5)$P_3$ are inorganic phosphate and Ins(1,4)$P_2$. There is no electron density evident for inorganic phosphate, suggesting that inorganic phosphate dissociates from SPsynaptojanin-IPP5C under the conditions used. Ins(1,4)$P_2$ remains bound, but in contrast to APE1, where flanking DNA sequences tightly constrain the binding mode of the nicked product, the binding of the Ins(1,4)$P_2$ product appears to be less constrained.

The greatest puzzle of inositol kinase and phosphatase enzymology concerns the origin of phosphorylation and dephosphorylation site selectivity. 5-phosphatases are competent to bind soluble and lipid inositol derivatives phosphorylated at combinations of the 3, 4, and 5 positions, yet they dephosphorylate only the 5-position. In the absence of a structural comparison between reactive and unreactive complexes, the mechanism of site

Table 1. Enzyme Activity of SPsynaptojanin IPP5C Mutants

| | No Detergent | | | 0.2% Triton X-100 | | | | |
|---|---|---|---|---|---|---|---|---|
| | PI(3,5)$P_2$ | PI(4,5)$P_2$ | $PIP_3$ | PI(3,5)$P_2$ | PI(4,5)$P_2$ | $PIP_3$ | $IP_3$ | $IP_4$ |
| IPP5C | 100 | 100 | 100 | ND | 100 | 100 | 100 | 100 |
| IPP5C$^{D838G}$ | ND | 1 | ND | ND | ND | ND | ND | ND |
| IPP5C$^{K795R,R810N}$ | 50 | 5 | 10 | ND | 0.1 | 1 | ND | ND |
| IPP5C$^{K669E,K808E}$ | ND | 10 | 1 | ND | 10 | 1 | 1 | ND |
| IPP5C$^{K669E,K808N}$ | ND | 10 | 1 | ND | 20 | 10 | 10 | ND |

The mutant activity values are expressed for each substrate as percent maximal activity relative to SPsynaptojanin IPP5C (assigned a maximal value of 100%). ND: not detected.

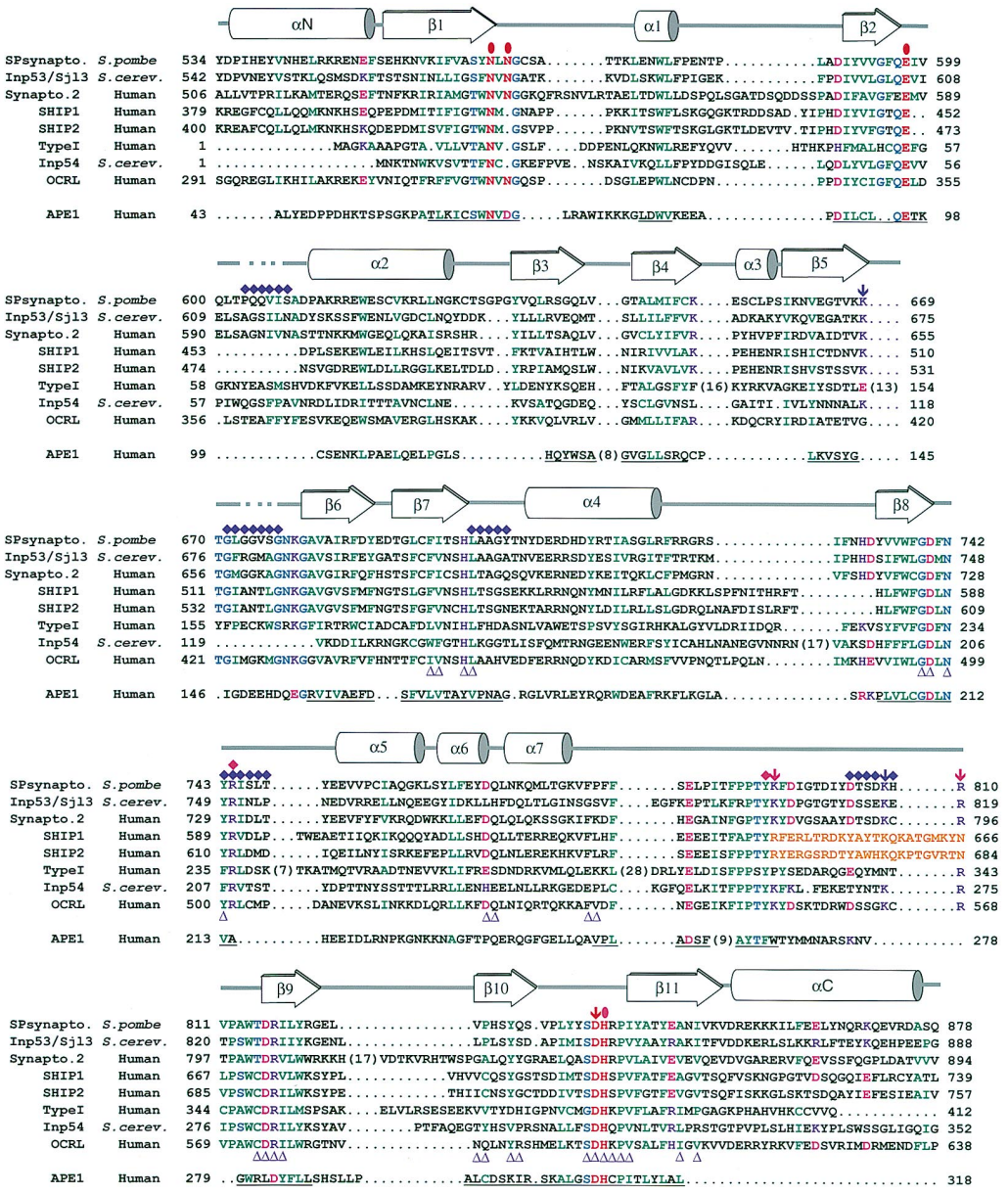


Figure 6. Sequence Alignment of SPsynaptojanin-IPP5C, Other Representative 5-Phosphatases, and Structure-Based Alignment of APE1

Disordered regions in the SPsynaptojanin-IPP5C structure are marked by dashed lines. Catalytic and divalent metal binding residues are highlighted in orange. Conserved charged residues highlighted in magenta (acidic) and purple (basic), and conserved hydrophobic residues are highlighted in green. Other conserved residues are highlighted in blue. The unique insertion implicated in 3-phosphoinositide specificity of SHIP1 and SHIP2 is highlighted in yellow. Residues coordinating to the active site metal ion either directly or through water molecules are marked with orange ellipses. Residues involved in direct phosphoinositide binding are marked by magenta symbols, arrows for those mutated in this study, diamonds for others. Residues on the putative membrane binding face are marked by purple symbols, arrows for those mutated in this study, diamonds for others. The active site Asp-838 mutated in the study is marked with an orange arrow. Loci of OCRL disease mutants are marked by purple triangles underneath the corresponding residues.

selectivity has been obscure. The active sites of SPsynaptojanin-IPP5C and APE1 are so similar that it is reasonable to assume that the 5-phosphoryl of SPsynaptojanin-IPP5C's substrates binds in the same geometry as the scissile phosphate of APE1, providing a model for the reactive complex. The Ins(1,4)$P_2$ complex reveals for the first time the structure of an unreactive inositol phosphate complex. The 4-phosphoryl is 4.6 Å away from the scissile phosphate in the APE1 pseudo-Michaelis complex. His-839 is 5.2 Å away from the closest oxygen atom of the 4-phosphoryl, while its counterpart His-309 is directly hydrogen bonded to the scissile phosphate in the APE1 complex with a distance of 2.7 Å. The 4.6 Å displacement of the 4-phosphoryl group from optimal dephosphorylation geometry satisfactorily explains why 5-phosphatases are not 4-phosphatases.

## Substrate Specificity Determinants

The SH2-domain-containing 5-phosphatases SHIP1 and SHIP2 are distinguished from all others by their

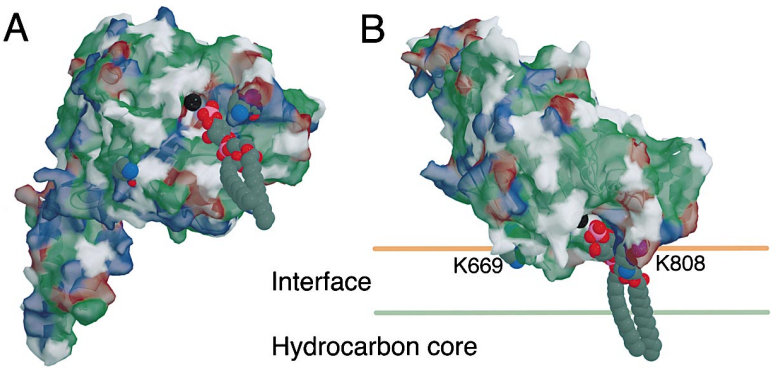


Figure 7. Membrane Docking of SPsynaptojanin-IPP5C

(A) Molecular surface of SPsynaptojanin-IPP5C, colored blue (basic), red (acidic), green (hydrophobic), and white (uncharged polar). Atoms are colored blue (nitrogen), red (oxygen), gray (carbon), lavender (phosphorous), and black (calcium). The surface is viewed looking directly upward from the putative plane of the membrane.

(B) Surface of SPsynaptojanin-IPP5C docked to a membrane, with the polar interface and hydrophobic core regions of the membrane shown to scale. The two membrane-interface side chains mutated in this study are highlighted in an all atom space-filling representation, and a dimyristoyl tail has been modeled onto the Ins(1,4)$P_2$ headgroup to provide a model for membrane-associated PI(4)P bound to the enzyme.

strong preference for D-3 inositol phosphate substrates. These enzymes are the focus of intensive study because of their role in signaling in the immune system and in downregulating insulin response. The latter function has made SHIP2 a potentially attractive target for drug design directed at type II diabetes, and adds urgency to identifying the determinants of D-3 specificity.

To identify potential substrate specificity determinants, the sequence conservation of inositol phosphate binding residues was examined to determine which residues were conserved in the SHIP subgroup but diverged in other sequences (Figure 6). Only two residues of SPsynaptojanin fit this criterion, Lys-795 (Arg in SHIP2) and Arg-810 (Asn in SHIP2). Therefore, the mutant K795R/R810N was constructed and characterized. This mutant had 2-fold reduced activity toward PI(3,5)$P_2$, as compared to 20-fold reduced activity vs. PI(4,5)$P_2$. The mutant has 10-fold reduced activity toward $PIP_3$ as compared to wild-type; however, the interpretation of this result is complicated by the presentation of $PIP_3$ to the enzyme in pure synthetic vesicles as compared to presentation in yeast membranes in the case of PI(3,5)$P_2$ and PI(4,5)$P_2$. The precise mechanism of selectivity could be based on modulation of either affinity or catalytic geometry by these two amino acids, and its clarification awaits further study. Nevertheless, we have been able to pinpoint key determinants for substrate specificity and engineer a 5-phosphatase with altered specificity based on structural analysis. Such engineered 5-phosphatases may prove to be valuable reagents for understanding the relative roles of the various 5-phosphatase dephosphorylation reactions in vivo. Pending the structure determination of SHIP2, engineered 5-phosphatase mutants may also provide a useful starting point for structure-based inhibitor design.

### Model for Membrane and Inositol Phosphate Binding

The identification of the active site provides a powerful constraint on the possible modes of membrane interaction. The surface surrounding the active site is formed primarily by loops associated with sheet II, including $\beta$7-$\alpha$4, $\beta$8-$\alpha$5, and $\alpha$7-$\beta$9. Parts of two other loops in this region are invisible in the electron density and therefore presumed to be disordered in the absence of membrane interaction: residues 603–607 of the $\beta$2-$\alpha$2 segment and residues 673–676 of the $\beta$5-$\beta$6 segment. The N-terminal portions of the $\alpha$ helices 4 and 5 also participate in this part of the molecular surface. It is possible that the partial positive charges at the helix N termini participate in interactions with anionic lipid headgroups. The molecular surface surrounding the active site is relatively flat (Figure 7), resembling that of another key enzyme in inositol lipid turnover, phosphatidylinositol phosphate kinase (PIPK; Rao et al., 1998; Hurley et al., 2000). In contrast to PIPK, there is relatively little concentration of positive charge in the flat surface, except in the active site itself. This argues that the activity of SPsynaptojanin-IPP5C against membrane substrates might depend more on the absence of steric interference with membrane binding than on electrostatic attraction between the enzyme and the membrane.

Type I 5-phosphatase is distinguished by its inability to dephosphorylate membrane bound inositol phosphates. We pinpointed two basic residues on the putative membrane binding face of SPsynaptojanin-IPP5C that are conserved in most 5-phosphatases but not in type I. These residues are Lys-669 and Lys-808 in SPsynaptojanin-IPP5C, and in the type I enzyme they are replaced by Glu and Asn, respectively. Lys-669 is remote from the active site, while Lys-808 is in the active site region, although not in direct contact with Ins(1,4)$P_2$ in the complex structure. The type I-like mutant K669E/K808N and a mutant designed to more drastically interfere with electrostatic membrane binding, K669E/K808E, were constructed. These mutants exhibited sharply decreased activity against lipid substrates, as well as decreased activity toward soluble substrates (Table 1). These results suggest that one or both of these residues, most likely Lys-808, make contact with the substrate in the reactive complex, even though they do not make contact in the product complex. The results also suggest that other regions of the protein must be involved in selectivity for lipid vs. soluble substrates. In addition to the absence of two basic residues noted above, the type I sequence is distinguished from the other 5-phosphatases by several large insertions in their IPP5C domain. Three of these insertions are in the putative membrane binding loops $\beta$5-$\beta$6, $\beta$8-$\alpha$5, and $\alpha$7-$\beta$9 (Figure 6). The steric bulk of these insertions could interfere with binding to the membrane surface.

Table 2. Crystallographic Analysis

| | | | | | | | | | |
|---|---|---|---|---|---|---|---|---|---|
| **Data collection statistics** | | | | | | | | | |
| Crystals | | | Native | | I | | Ca +$IP_3$ | | |
| Maximum resolution (Å) | | | 2.0 | | 1.9 | | 1.8 | | |
| Number of observed reflections | | | 117,178 | | 281,277 | | 148,755 | | |
| Number of unique reflections | | | 32,930 | | 38,646 | | 44,082 | | |
| Completeness (%)[a] | | | 99.3 (96.5) | | 97.9 (89.2) | | 95.6 (82.4) | | |
| $R_{sym}$[b] (%) | | | 3.9 (16.1) | | 5.4 (16.1) | | 3.8 (14.5) | | |
| Mean $I/\sigma(I)$ | | | 17.0 | | 16.7 | | 17.8 | | |
| **SIRAS phasing statistics** | | | | | | | | | |
| Number of sites | | | | | 5 | | | | |
| Resolution limits (Å) | | | | | 30–2.0 | | | | |
| $d_{min}$ (Å) | Total | 8.0 | 5.0 | 4.6 | 4.0 | 3.6 | 3.3 | 3.0 | 2.8 |
| Phasing power (acentric) | 1.03 | 2.16 | 1.90 | 1.21 | 0.95 | 0.86 | 0.82 | 0.91 | 0.90 |
| $R_{cullis}$ (centric) | 0.61 | 0.55 | 0.55 | 0.67 | 0.56 | 0.65 | 0.71 | 0.66 | 0.58 |
| Figure of merit | 0.37 | 0.38 | 0.43 | 0.39 | 0.34 | 0.24 | 0.36 | 0.39 | 0.41 |
| **Refinement statistics** | | | | | | | | | |
| Resolution limits (Å) | | | | | 30–2.0 | | 32–1.8 | | |
| Number of reflections | | | | | 31,846 | | 43,044 | | |
| $R$ factor[c] (%) | | | | | 19.5 | | 19.1 | | |
| $R_{free}$[c] (%) | | | | | 22.5 | | 21.8 | | |
| No. of protein/solvent/ligand atoms | | | | | 2,766/186/0 | | 2,766/224/21 | | |
| Rmsd from ideal bond length (Å) | | | | | 0.018 | | 0.022 | | |
| Rmsd from ideal bond angle (°) | | | | | 1.94 | | 2.14 | | |

[a] Numbers in parentheses refer to the respective highest resolution data shell in each dataset.
[b] $R_{sym} = \Sigma_h\Sigma_i|I_i(h) - <I(h)>|/\Sigma_h\Sigma_i I_i(h)$; $I_i(h)$ is the $i$th measurement of reflection $h$ and $<I(h)>$ is the weighted mean of all measurements of $I(h)$.
[c] $R$ factor $= \Sigma_h||F_{obs}(h)| - |F_{calc}(h)||/\Sigma_h|F_{obs}(h)|$; $R_{free}$ is calculated with 10% of the data.

### Conserved Motifs in 5-Phosphatases and Missense Mutations in Lowe's Oculocerebrorenal Dystrophy

Two consensus sequence motifs are a defining feature of the 5-phosphatase family (Jefferson and Majerus, 1996). These are WXGDXN(Y/F)R and P(A/S)W(C/T)DRIL, corresponding to SPsynaptojanin residues 737–744 and 812–819, respectively. The conservation of these residues is explainable based on the SPsynaptojanin-IPP5C structure. The Gly of the first motif (SPsynaptojanin 739) has the conformation ($\phi = 141, \psi = -157$), which is disallowed for non-Gly residues. The Gly is presumably in this conformation in order to position the immediately C-terminal Asp. Asp-740 is adjacent to the catalytic His-839 but does not form a hydrogen bond with the His. Rather, it is positioned to act as a catalytic base in the dephosphorylation reaction. A key role in catalysis is consistent with the total loss of catalytic activity observed for the corresponding D476A mutant of platelet 75 kDa inositol polyphosphatase II (5-phosphatase II). The Asn in consensus position 6 of the first motif (SPsynaptojanin 742) stabilizes Arg-744. This Arg, consensus position 8, directly interacts with Ins(1,4)$P_2$. Roles of the Asn and Arg in the active site are consistent with the complete or near complete loss of activity in the corresponding N478A and R480A mutants of 5-phosphatase II (Jefferson and Majerus, 1996).

In the second motif, consensus position 4 can be a Cys or Thr. In SPsynaptojanin, this corresponds to Thr-815. Thr-815 directly interacts with His-839 from the side opposite to Asp-740 in motif 1. Asp-816 forms a hydrogen bond with the catalytic His-839, implicating the Asp directly in catalysis. Arg-817 in consensus position 6 is not part of the active site, but rather participates in a buried charge and hydrogen bonding network with Asp-768, Glu-785, and Tyr-829. The aromatic residues of both motifs and the Ile and Leu of the second motif are involved in the structure of the hydrophobic core, but not directly part of the active site. The lack of a direct binding role is consistent with the normal $K_m$ of the corresponding 5-phosphatase II mutants W551A and I555A (Jefferson and Majerus, 1996). These two residues are part of the hydrophobic core, and the reduced $V_m$ of these mutant enzymes could be due to loss of activity of a portion of the enzyme due to protein unfolding in the course of the enzyme assay.

A large number of mutations have been characterized in Lowe's patients (http://www.nhgri.nih.gov/DIR/GDRB/Lowe/ocrl1_mutations.html), including missense mutations in the codons for 14 different amino acid residues within the IPP5C domain of the OCRL1 protein. Nearly all of the affected residues are identical in SPsynaptojanin, and all but one of the remainder are conservative substitutions. Thus, the SPsynaptojanin-IPP5C structure can be used to understand the structural basis for this genetic disease. Only one mutation is difficult to map onto the SPsynaptojanin-IPP5C structure, a Val that corresponds to an insertion between residues 824 and 825 of SPsynaptojanin. The remainder of the mutations can be divided among those that directly impair binding and catalysis, and those that alter stability by disrupting the hydrophobic core or the polar Asp/Asp/Arg/Tyr core.

### Conclusions

The structure of the SPsynaptojanin-IPP5C domain reveals how a conserved DNase-like catalytic core has been expanded to yield a diverse family of inositol polyphosphate signaling enzymes. Variations in the surface surrounding the active site contribute to specificity for

lipid versus soluble inositol polyphosphates. Differences in the α7-β9 loop appear to be primarily responsible for differences in preferences for 3-phosphorylated versus other substrates. This information provides new avenues to manipulate the signaling specificity of 5-phosphatases as probes for their cellular function. The structure also allows an understanding of the molecular mechanisms whereby missense mutations in genes coding for 5-phosphatases can lead to disease. Finally, the first structure of an IPP5C domain provides a starting point for structure-based inhibitor design against such potential therapeutic targets as SHIP2.

## Experimental Procedures

### Protein Expression and Purification

DNA coding for *S. pombe* SPsynaptojanin residues 534–880 was amplified by PCR using *S. pombe* cosmid c2G2 as a template and subcloned into the BamHI and EcoRI sites of a modified pET22b vector (Sheffield et al., 1999) containing a TEV protease cleavage site. Site-directed mutations were introduced by PCR using the QuikChange method (Stratagene). The $His_6$-tagged protein was expressed in *Escherichia coli* BL21 (DE3) cells (Novagen); SPsynaptojanin-IPP5C domain was purified from the lysate using Ni-NTA resin (Qiagen), and cleaved by incubation with TEV protease (Life Technologies). The cleaved $His_6$ tag and $His_6$-tagged TEV protease were removed by Ni-NTA resin. The protein yield was 80 mg $L^{-1}$ bacterial culture.

### 5-Phosphatase Activity Assay

The activity toward [$^3$H]-*myo*-inositol-labeled yeast substrate was carried out as described (Guo et al., 1999). 3-phosphorylated lipid substrates were prepared with purified p110 PI 3-kinase subunit (generous gift from Lewis Cantley). The activity toward soluble inositol substrates was analyzed as described (Spiegelberg et al., 1999). The formate buffer for $IP_3$ assay consisted of 0.35 M $NH_4COO$ and 0.01 M COOH; the buffer for the IP4 assay consisted of 0.55 M $NH_4COO$ and 0.05 M COOH. Substrate I(1,4,5,6)$P_4$ was prepared as described (Odom et al., 2000).

### Yeast In Vivo Experiments

SPsynaptojanin-IPP5C wild-type and mutant DNAs were subcloned into pUNI-10 using the NcoI and SalI sites (Liu et al., 1998). The resultant pUNI-SPsynaptojanin-IPP5C vectors were then recombined with a modified pRS316 vector (Sikorski and Hieter, 1989) containing the copper inducible *CUP1* promoter, lox sites, and a myc3 N-terminal tag. These vectors were transformed into *inp51 inp52 inp53* GAL*::INP53* mutant yeast. The transformants were grown to saturation in media containing galactose, then serially diluted and spotted onto plates containing dextrose and varying concentrations of $CuSO_4$.

### Crystallization and Data Collection

Purified protein at 8 mg $ml^{-1}$ concentration was dialyzed against 150 mM NaCl, 20 mM Tris-HCl (pH 8.0), and 10 mM 2-mercaptoethanol at 4°C and crystals were grown in the dialysis bag over 20 hr. Crystals were cryoprotected in mother liquor supplemented with 25% glycerol and flash frozen under $N_2$ gas at 95 K. To prepare an iodide derivative, 150 mM potassium iodide was included in cryoprotectant (Dauter et al., 2000). For the $Ca^{2+}$-Ins(1,4)$P_2$ complex, a crystal was soaked in dialysis buffer containing 1 mM $CaCl_2$ and 2 mM Ins(1,4,5)$P_3$. The crystals are of space group C2 with a = 149.0 Å, b = 67.5Å, c = 51.5 Å, and β = 106.2°. All diffraction data used in the structure determination (Table 2) were collected on an RAXIS IV imaging plate detector with Cu Kα radiation (RIGAKU, Tokyo). Data were processed with HKL (Otwinowski and Minor, 1997).

### Structure Determination and Refinement

Five iodide sites were located using automated Patterson search and cross-validation in SOLVE (Terwilliger and Berendzen, 1996). Heavy atom parameters were refined with SOLVE and subsequently in SHARP (de la Fortelle and Bricogne, 1997). Phases were improved with density modification in SOLOMON (Abrahams and Leslie, 1996). The model was built into a 2.8 Å electron density map with O (Jones et al., 1991). Model refinement was carried out with CNS (Brünger et al., 1998) using torsional dynamics and the maximum likelihood target function and all measured data from the native set to 2.0 Å resolution and Ca-Ins(1,4)$P_2$-complex set to 1.8 Å resolution. The refinement was monitored using the free R factor calculated with 10% of observed reflections. The refined crystal structure includes residues 534–878 of SPsynaptojanin and 186 water molecules for the native model, and residues 534–878 of SPsynaptojanin, 1 Ins(1,4)$P_2$ molecule, 1 calcium ion, and 224 water molecules for the $Ca^{2+}$-Ins(1,4)$P_2$-complex model. The structures were analyzed using PROCHECK (Laskowski et al., 1993). 89.2% and 90.2% of the residues in native model and in the Ca-Ins(1,4)$P_2$-complex model, respectively, fall in most favored regions. Only one residue, Val-644, falls in the disallowed regions of the Ramachandran plot. Val-644 is on the border of the disallowed region, and as this residue is in a region of excellent electron density, we are confident its conformation is modeled correctly.

## Acknowledgments

We thank Z. Dauter and B. Canagarajah for assistance with data collection at beamline X9B, National Synchrotron Light Source, Brookhaven National Laboratories; M. Pearson, B. Miller, and C. Heaton at beamline F2, CHESS; L. Cantley (Harvard Medical School, Boston, MA) for kindly providing recombinant PI3Kinase; R. Gwilliam (The Sanger Centre,UK) for providing the *S. pombe* cosmid; and A. Hickman for comments on the manuscript.

Received February 21, 2001; revised March 26, 2001.

## References

Abrahams, J.P., and Leslie, A.G.W. (1996). Methods used in the structure determination of bovine F-1 ATPase. Acta Crystallogr. D *52*, 30–42.

Altschul, S.F., Madden, T.L., Schäffer, A.A., Zhang, J., Zhang, Z., Miller, W., and Lipman, D.J. (1997). Gapped BLAST and PSI-BLAST: a new generation of protein database search programs. Nucleic Acids Res. *25*, 3389–3402.

Attree, O., Olivos, I.M., Okabe, I., Bailey, L.C., Nelson, D.L., Lewis, R.A., McInnes, R.R., and Nussbaum, R.L. (1992). The Lowe's oculocerebrorenal syndrome gene encodes a protein highly homologous to inositol polyphosphate-5-phosphatase. Nature *358*, 239–242.

Bateman, A., Birney, E., Durbin, R., Eddy, S.R., Finn, R.D., and Sonnhammer, E.L. (1999). Pfam 3.1: 1313 multiple alignments match the majority of proteins. Nucleic Acids Res. *27*, 260–262.

Berridge, M.J., and Irvine, R.F. (1989). Inositol phosphates and cell signaling. Nature *341*, 197–205.

Brünger, A.T., Adams, P.D., Clore, G.M., DeLano, W.L., Gros, P., Grosse-Kunstleve, R.W., Jiang, J.S., Kuszewski, J., Nilges, M., Pannu, N.S., et al. (1998). Crystallography and NMR system (CNS): a new software system for macromolecular structure determination. Acta Crystallogr. D *54*, 905–921.

Clement, S., Krause, U., Desmedt, F., Tanti, J.-F., Behrends, J., Pesesse, X., Sasaki, T., Penninger, J., Doherty, M., Malaisse, W., et al. (2001). The lipid phosphatase SHIP2 controls insulin sensitivity. Nature *409*, 92–96.

Cremona, O., Di Paolo, G., Wenk, M.R., Luthi, A., Kim, W.T., Takei, K., Daniell, L., Nemoto, Y., Shears, S.B., Flavell, R.A., et al. (1999). Essential role of phosphoinositide metabolism in synaptic vesicle recycling. Cell *99*, 179–188.

Dauter, Z., Dauter, M., and Rajashankar, K.R. (2000). Novel approach to phasing proteins: derivatization by short cryo-soaking with halides. Acta Crystallogr. D *56*, 232–237.

De Camilli, P., Emr, S.D., McPherson, P.S., and Novick, P. (1996). Phosphoinositides as regulators in membrane traffic. Science *271*, 1533–1539.

de La Fortelle, E., and Bricogne, G. (1997). Maximum-likelihood

heavy-atom parameter refinement for multiple isomorphous replacement and multiwavelength anomalous diffraction methods. Methods Enzymol. *276*, 472–494.

Dlakic, M. (2000). Functionally unrelated signalling proteins contain a fold similar to Mg2+-dependent endonucleases. Trends Biochem. Sci. *25*, 272–273.

Drayer, A.L., Pesesse, X., De Smedt, F., Communi, D., Moreau, C., and Erneux, C. (1996). The family of inositol and phosphatidylinositol polyphosphate 5-phosphatases. Biochem. Soc. Trans. *24*, 1001–1005.

Gibrat, J.-F., Madej, T., and Bryant, S.H. (1996). Surprising similarities in structure comparison. Curr. Opin. Struct. Biol. *6*, 377–385.

Gorman, M.A., Morera, S., Rothwell, D.G., de la Fortelle, E., Mol, C.D., Tainer, J.A., Hickson, I.D., and Freemont, P.S. (1997). The crystal structure of the human DNA repair endonuclease HAP1 suggests the recognition of extra-helical deoxyribose at DNA abasic sites. EMBO J. *16*, 6548–6558.

Guo, S., Stolz, L.E., Lemrow, S.M., and York, J.D. (1999). SAC1-like domains of yeast SAC1, INP52, and INP53 and of human synaptojanin encode polyphosphoinositide phosphatases. J. Biol. Chem. *274*, 12990–12995.

Harris, T.W., Hartwieg, E., Horvitz, H.R., and Jorgensen, E.M. (2000). Mutations in synaptojanin disrupt synaptic vesicle recycling. J. Cell Biol. *150*, 589–599.

Hermosura, M.C., Takeuchi, H., Fleig, A., Riley, A.M., Potter, B.V.L., Hirata, M., and Penner, R. (2000). $InsP_4$ facilitates store-operated calcium influx by inhibition of $InsP_3$ 5-phosphatase. Nature *408*, 735–740.

Hurley, J.H., Tsujishita, Y., and Pearson, M.A. (2000). Floundering about at cell membranes: A structural view of phospholipid signaling. Curr. Opin. Struct. Biol. *10*, 737–743.

Jefferson, A.B., and Majerus, P.W. (1996). Mutation of the conserved domains of two inositol polyphosphate 5-phosphatases. Biochemistry *35*, 7890–7894.

Jones, T.A., Zou, J.Y., Cowan, S.W., and Kjeldgaard, M. (1991). Improved methods for building protein models in electron density maps and the location of errors in these models. Acta Crystallogr. A *47*, 110–119.

Kisseleva, M.V., Wilson, M.P., and Majerus, P.W. (2000). The isolation and characterization of a cDNA encoding phospholipid-specific inositol polyphosphate 5-phosphatase. J. Biol. Chem. *275*, 20110–20116.

Kraulis, P. (1991). MOLSCRIPT: a program to produce both detailed and schematic plots of protein structures. J. Appl. Crystallogr. *24*, 946–950.

Laskowski, R.A., MacArthur, M.W., Moss, D.S., and Thornton, J.M. (1993). PROCHECK: a program to check the stereochemical quality of protein structures. J. Appl. Crystallogr. *24*, 946–950.

Liscovitch, M., and Cantley, L.C. (1994). Lipid second messengers. Cell *77*, 329–334.

Liu, Q., Li, M.Z., Leibham, D., Cortez, D., and Elledge, S.J. (1998). The univector plasmid-fusion system, a method for rapid construction of recombinant DNA without restriction enzymes. Curr. Biol. *8*, 1300–1309.

Majerus, P.W. (1992). Inositol phosphate biochemistry. Annu. Rev. Biochem. *61*, 225–250.

Majerus, P.W., Kisseleva, M.V., and Norris, F.A. (1999). The role of phosphatases in inositol signaling reactions. J. Biol. Chem. *274*, 10669–10672.

Matsuo, Y., Yamada, A., Tsukamoto, K., Tamura, H.-O., Ikeawa, H., Nakamura, H., and Nishikawa, K. (1996). A distant evolutionary relationship between bacterial sphingomyelinase and mammalian DNase I. Prot. Sci. *5*, 2459–2467.

McPherson, P.S., Garcia, E.P., Slepnev, V.I., David, C., Zhang, X., Grabs, D., Sossin, W.S., Bauerfeind, R., Nemoto, Y., and De Camilli, P. (1996). A presynaptic inositol-5-phosphatase. Nature *379*, 353–357.

Merritt, E.A., and Bacon, D.J. (1997). Raster3D version 2.0: A program for photorealistic molecular graphics. Methods Enzymol. *277*, 505–524.

Mitchell, C.A., Brown, S., Campbell, J.K., Munday, A.D., and Speed, C.J. (1996). Regulation of second messengers by the inositol polyphosphate 5-phosphatases. Biochem Soc Trans. *24*, 994–1000.

Mol, C.D., Kuo, C.-F., Thayer, M.M., Cunningham, R.P., and Tainer, J.A. (1995). Structure and function of the multifunctional DNA-repair enzyme exonuclease III. Nature *374*, 381–386.

Mol, C.D., Izumi, T., Mitra, S., and Tainer, J.A. (2000). DNA-bound structures and mutants reveal abasic DNA binding by APE1 DNA repair and coordination. Nature *403*, 451–456.

Odom, A.R., Stahlberg, A., Wente, S.R., and York, J.D. (2000). A role for nuclear inositol 1,4,5-trisphosphate kinase in transcriptional control. Science *287*, 2026–2029.

Odorizzi, G., Babst, M., and Emr, S.D. (2000). Phosphoinositide signaling and the regulation of membrane trafficking in yeast. Trends Biochem. Sci. *25*, 229–235.

Ono, M., Okada, H., Bolland, S., Yanagi, S., Kurosaki, T., and Ravetch, J.V. (1997). Deletion of SHIP or SHP-1 reveals two distinct pathways for inhibitory signaling. Cell *90*, 293–301.

Otwinowski, Z., and Minor, W. (1997). Processing of X-ray diffraction data collected in oscillation mode. Methods Enzymol. *276*, 307–326.

Rameh, L.E., and Cantley, L.C. (1999). The role of phosphoinositide 3-kinase lipid products in cell function. J. Biol. Chem. *274*, 8347–8350.

Rao, V.D., Misra, S., Boronenkov, I.V., Anderson, R.A., and Hurley, J.H. (1998). Structure of type IIβ phosphatidylinositol phosphate kinase: A protein kinase fold flattened for interfacial phosphorylation. Cell *94*, 829–839.

Schultz, J., Milpetz, F., Bork, P., and Ponting, C.P. (1998). SMART, a simple modular architecture research tool: Identification of signaling domains. Proc. Natl. Acad. Sci. USA *95*, 5857–5864.

Shears, S.B. (1998). The versatility of inositol phosphates as cellular signals. BBA Mol. Cell. Biol. Lipids *1436*, 49–67.

Sheffield, P., Garrard, S., and Derewenda, Z. (1999). Overcoming expression and purification problems of RhoGDI using a family of parallel expression vectors. Protein Expr. Purification *15*, 34–39.

Sikorski, R.S., and Hieter, P. (1989). A system of shuttle vectors and yeast host strains designed for efficient manipulation of DNA in Saccharomyces cerevisiae. Genetics *122*, 19–27.

Spiegelberg, B.D., Xiong, J.P., Smith, J.J., Gu, R.F., and York, J.D. (1999). Cloning and characterization of a mammalian lithium-sensitive bisphosphate 3′-nucleotidase inhibited by inositol 1,4-bisphosphate. J. Biol. Chem. *274*, 13619–13628.

Srinivasan, S., Seaman, M., Nemoto, Y., Daniell, L., Suchy, S.F., Emr, S., De Camilli, P., and Nussbaum, R. (1997). Disruption of three phosphatidylinositol-polyphosphate 5-phosphatase genes from Saccharomyces cerevisiae results in pleiotropic abnormalities of vacuole morphology, cell shape, and osmohomeostasis. Eur. J. Cell Biol. *74*, 350–360.

Stolz, L.E., Huynh, C.V., Thorner, J., and York, J.D. (1998). Identification and characterization of an essential family of inositol polyphosphate 5-phosphatases (INP51, INP52 and INP53 gene products) in the yeast Saccharomyces cerevisiae. Genetics *148*, 1715–1729.

Suchy, S.F., Olivos-Glander, I.M., and Nussbaum, R.L. (1995). Lowe syndrome, a deficiency of a phosphatidylinotiol 4,5-bisphosphate 5-phosphatase in the Golgi apparatus. Hum. Mol. Genet. *4*, 2245–2250.

Suck, D., and Oefner, C. (1986). Structure of DNase I at 2.0 Å resolution suggests a mechanism for binding to and cutting DNA. Nature *321*, 620–625.

Terwilliger, T.C., and Berendzen, J. (1996). Correlated phasing of multiple isomorphous replacement data. Acta Crystallogr. D *52*, 749–757.

Whisstock, J.C., Romero, S., Gurung, R., Nandurkar, H., Ooms, L.M., Bottomley, S.P., and Mitchell, C.A. (2000). The inositol polyphosphate 5-phosphatases and the apurinic/apyrimidinic base excision repair endonucleases share a common mechanism for catalysis. J. Biol. Chem. *275*, 37055–37061.

Woscholski, R., and Parker, P.J. (1997). Inositol lipid 5-phosphatases—traffic signals and signal traffic. Trends Biochem. Sci. *22*, 427–431.

Zhang, X., Jefferson, A.B., Auethavekait, V., and Majerus, P.W. (1995). The protein deficient in Lowe syndrome is a phosphatidylinositol-4,5-bisphosphate 5-phosphatase. Proc. Natl. Acad. Sci. USA *92*, 4853–4856.

**Accession Numbers**

Coordinates have been deposited in the Protein Data Bank at the RCSB with the accession codes 1I9Y and 1I9Z for the apo and complex structures, respectively.